

Article

Analysis of a Combined Solar Drying System for Wood-Chips, Sawdust, and Pellets

Baibhaw Kumar , Gábor Szepesi , Zoltán Szamosi  and Gyula Krámer

Institute of Energy Engineering and Chemical Machinery, University of Miskolc, 3515 Miskolc, Hungary

* Correspondence: vegybk@uni-miskolc.hu

Abstract: The future of conventional fuels has limited sustainability and creates disquietude because of the ubiquitous energy crisis worldwide. The judicious use of biomass or wood-based fuels is inevitable. The quality of wood fuels depends on the moisture content, and subsequently, solar drying solutions can play a vital role in adequately storing and controlling moisture in the fuels. In the present study, a novel forced convection cabinet-type solar dryer was developed and investigated for its thermal performance. An artificial neural network (ANN model) was created to predict the final moisture content of the drying system. The drying behavior of three distinct wood fuels, i.e., woodchips, sawdust, and pellets, was kept under observation to plot the drying curve based on their calculated moisture ratio. The dryer reached a maximum temperature of 60 °C while maintaining a temperature gradient of 10–20 °C. The maximum thermal energy and exergy efficiency was recorded as 55% and 51.1%, respectively. The ANN-optimized model was found suitable with reasonable values of coefficient of correlation (R) for the model.

Keywords: solar drying; woodchips; sawdust; pellets; artificial neural network



Citation: Kumar, B.; Szepesi, G.; Szamosi, Z.; Krámer, G. Analysis of a Combined Solar Drying System for Wood-Chips, Sawdust, and Pellets. *Sustainability* **2023**, *15*, 1791. <https://doi.org/10.3390/su15031791>

Academic Editor: Marzena Smol

Received: 19 December 2022

Revised: 10 January 2023

Accepted: 16 January 2023

Published: 17 January 2023



Copyright: © 2023 by the authors. Licensee MDPI, Basel, Switzerland. This article is an open access article distributed under the terms and conditions of the Creative Commons Attribution (CC BY) license (<https://creativecommons.org/licenses/by/4.0/>).

1. Introduction

Biomass fuels will play a vital role in energy consumption scenarios of the future. Researchers worldwide are examining the efficiency and utility of renewable energy sources for large-scale utility. Wood fuels will be critical in the energy transition from conventional to renewable energy sources. A reasonable strategy comprising the growth, stock, usage, pricing, and efficient mobility of wood fuel feedstock is inevitable in future energy transitions [1]. The storage and optimal utilization of woody biomass are energy intensive. The calorific value of the wood fuel governs the efficiency of its thermal performance as a fuel. The various stages of this fuel production and storage in the form of woodchips, sawdust, or pellets require drying for moisture removal [2]. Thermochemical properties, for example, moisture content, and chemical compositions influence the heating value of the fuel [3]. In large-scale usage, the consequences could primarily affect the efficiency of energy-producing systems, such as boiler plants. Henceforth, there is a compelling requirement for low-cost and highly efficient drying technologies for wood biomass [4]. The wood industry is a foundational sector that provides raw materials to manufacture several biofuels. The last ten years have seen a significant increase in competition on the global market for wood products such as woody biofuels. As a result, manufacturers and producers are always looking for ways to increase their production process efficiency. Traditional facilities now have a statistically lower opportunity to be converted into automated manufacturing facilities to boost productivity. This opportunity is made possible by recent advancements in automation systems and manufacturing technology [5]. A study suggests the drying process covers almost 70% of the energy utilized by wood producers [6]. Conventional drying based on traditional fossil fuels is the predominant drying technique in the wood business. In the last 10 years, interest in solar energy as a substitute for dry wood has grown. Several experimental investigations and numerical studies have been published in

the recent literature where the authors classified the solar wood dryers into four categories. Figure 1. shows the classification of solar wood dryers and their characteristic feature [7].

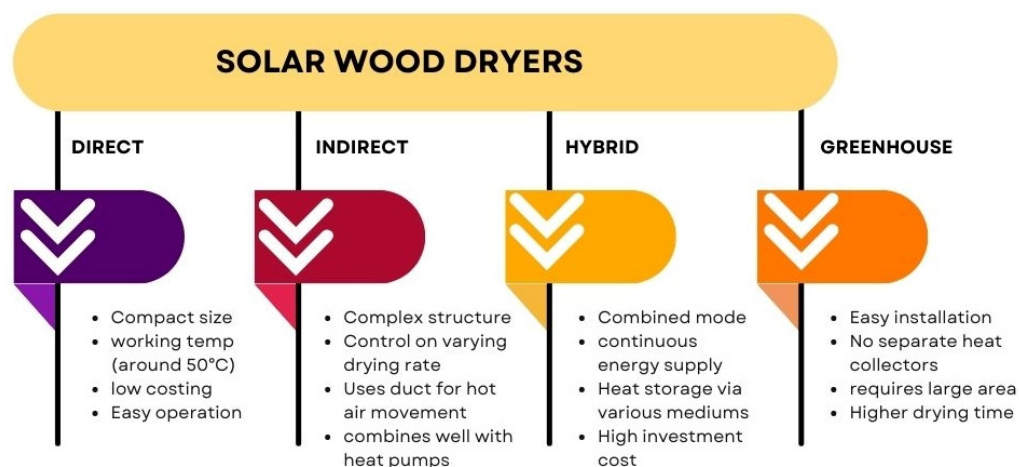


Figure 1. Classification of solar wood dryers and their characteristics based on a review study from Lamrani et al. [7].

It is noticeable that 20% of all published papers over the past ten years have come from China and France. India ranked third for solar wood drying, followed in order by Canada, Morocco, and the United States. Commercialization of solar dryers is also increasing in the mentioned countries. Solar dryers, particularly for wood drying, can be majorly found in India [8], the USA [9], China [10], and Australia [11]. These technologies will make the wood fuel's overall utilization economically sound and provide long storage life. With proper business model analysis using a business canvas, entrepreneurship opportunities can be explored with solar driers [12]. Researchers have also compared the multimode drying units with commercially available systems. Such studies help in commercial validation of the design [13]. The literature suggests that the compounds in the woody biomass degrade due to chemical and biological processes during fuel storage in the form of wood chips or wood pellets [14]. The drying processes should be designed to reduce the negative impacts on fuel quality, human health, and environmental concerns. Wood fuels are commonly used in three different kinds, i.e., wood chips (chopped from huge wood logs), sawdust (granulated version of wood chips), and pellets (produced by compressing the sawdust fiber). In addition, the drying of these different forms of wood fuel varies with the requirements of the utility system. The mechanical properties of these wood fuels are also affected by the fluctuation in moisture content embodied in them. For instance, the moisture content in sawdust form influences the maximum shear stress, whereas no influence was observed for woodchips [15]. Such nuances associated with these fuels affect the designing of drying techniques for these fuels. Depending on the size and type of biofuel, different types of dryers are used for drying wood fuels. The rotary (operating temperature 250–400 °C) and flash dryers have been used since 1970 and 1980. Later, in the 1990s, superheated steam dryers (medium-pressure steam at about 20 bars) came into use [16]. However, the most commonly used dryers in the last two decades are moving bed dryers due to their cheaper cost, volume flexibility, and temperature control. Now, many researchers in the last few years also started to look for renewable drying solutions for the storage of wood chips. Solar energy has evolved as one of the promising futures for the drying application of various wood forms. Several patents and experimental investigations are being performed with different solar drying modules. Review work on solar wood dryers suggests that the investigators should consider the complex nature of wood drying. Instead of simple lumped modeling, multi-physical modeling should be considered [7]. Alberto et al. [17] performed a comparative study on open sun drying and solar greenhouse drying during the autumn season of pain. With 13.74 MJ/m² average

solar radiation, the wood chips achieved 10% relative humidity in 13 days. The greenhouse dryer reached 25.20 °C higher temperature and 20% less relative humidity than open sun drying. Hybrid solar dryers can even enhance the drying performance of woody biomass by 92% and reduce energy consumption by 85% [18]. However, such studies are case-dependent. Such results demonstrate the excellent utilization of solar dryers for wood fuel drying. Another wood fuel form is sawdust, critical in forming wood pellets. Recent advancements have been made in combining the solar drying of sawdust on spouted beds with phase change materials, which increased the drying air temperature by 10 °C [19]. The moisture content highly affects the quality, utility, and pricing of the widely used wood pellets. When *Acacia dealbata* was pelletized with solar drying, it was discovered that sawdust with a moisture level of 7% generated better-quality pellets with higher durability ratings and lower water resistance indices [20]. Researchers have investigated the drying of timber with different solar dryer designs. A study also investigated the potential of integrating sodium sulfate decahydrate ($\text{Na}_2\text{SO}_4 \cdot 10\text{H}_2\text{O}$) and sodium chloride (NaCl) as thermal storage for better efficiency [21]. Mathematical models and numerical calculations are standard for analyzing thermal efficiency [22]. The TRNSYS software package is used for simulation in solar drying of wood products [23]. Computational fluid dynamic (CFD) studies are proved helpful in such analysis [24].

As per the latest report from the United Nations Economic Commission for Europe (UNECE), In 2021, the European Union (EU) member states burned roughly 23.1 million tonnes of wood pellets. Because of the rising cost of fossil fuels and rising household demand, their consumption is anticipated to surpass 24 million tonnes in 2022 and continue to grow [25]. Trendline analysis based on solar irradiance shows that Hungary, as a central European country, has significant potential to harness solar energy [26]. The main form of wood-based biomass used by Hungary's heating plants is wood chips. This approach has difficulties because optimizing moisture content depends on storage, and moisture content strongly affects the value of the fuel. Henceforth, there is a dire need to maximize the efficiency of wood fuels through sustainable drying techniques. In our investigation, we focused on three primary wood fuels—woodchips, sawdust, and wood pellets. The energy exergy analysis is carried out, and an artificial neural network (ANN) model is presented to predict the final moisture content. A recent study shows photovoltaics and heat pump can be utilized for hybridization of the solar dryer for better energy efficiency [27]. This study proposes a hybrid drying system that combines a heat pump and a concentrated photovoltaic thermal. The development and validation of mathematical models for the transmission of mass and heat in the different dryer components were performed. In contrast, our work focuses on three different wood products (commonly used as biofuels) and their drying behavior. Additionally, instead of hybridization, we focus on a single heat source, i.e., solar thermal energy. We used a fan with an AC power supply to maintain the mass flow rate. The prime objectives of the study can be summarized as:

- To design and develop a lab-scale dryer for observing the drying behavior of woodchips, pellets, and sawdust in a combined dryer.
- To calculate the solar drying system's thermal energy, exergy, and overall efficiency.
- To develop an artificial neural network (ANN) model to predict the final moisture content for comparison with experimental results.
- To train, test, and validate the experimental data via MATLAB simulations for considering the efficiency of the design ANN model.

2. Materials and Methods

Due to their non-hygroscopic nature, wood biofuels cannot be 100% moisture free. However, solar drying can considerably reduce moisture, improving the properties of wood biofuels. Limited studies are available on the solar drying of wood-based biofuels (pellets, sawdust, and woodchips). In our present study, we investigate the drying behavior of biofuels in a combined solar dryer.

The methodology employed in this study included conceptualizing the structure of the forced convection solar dryer, designing the conceived dryer, building the designed dryer, and validating the experimental results with an artificial neural network tool. Energy and exergy analysis was performed for the drying system to evaluate its efficiency. Wood chips, pellets, and sawdust were utilized as the drying product under observation in the drying chamber with three different layers of tray.

2.1. Empirical Study on the Forced Convection Cabinet Solar Dryer

A forced convective cabinet solar dryer was prepared for this study at the University of Miskolc, Hungary. This dryer works on the indirect air circulation model, in which the hot air is collected in the air collector, as shown in the isometric view of the dryer in Figure 1. The dryer's body is made of wooden blocks, which are 2.5 cm thick and well-insulated on all sides. The size of the drying chamber (Length \times Breadth \times Height) is (80 \times 50 \times 45) cm. Thus, the total capacity of the dryer is 180,000 cm³, i.e., 180 L by volume. The drying cabinet consists of three trays separated by a distance of 7.5 cm. However, the pressure drop across the height was not considered while designing the drying system. On the top of the cabinet, a 50 cm long chimney is placed for the throughput of outlet air. The hot air solar collector attached to the dryer has an inclination of 40°. Transparent glass material is used for the air collector. For the air collector to provide ample air circulation and heat transfer, the length of the collector should be higher than its width [28]. The literature suggests the aspect ratio (length: width) be around 2 [29]. Based on (length \times width), i.e., (40 \times 60) cm, the aspect ratio of the proposed collector is 1.5. However, it can be improved further with size modification. The latitude angle (ϕ) of the location where drying is to be performed is generally very closely related to the angle of inclination of the collector (β) or the tilt angle, given that the collector's face must be facing south–north [29]. In general, the inclination angle is given as [30]:

$$\beta = \phi + 10^\circ \quad (1)$$

Based on the coordinates of the city of Miskolc, i.e., 48°06'15" N 20°47'30" E, the inclination angle was kept at 40° due to glass material size constraint. However, it can be improved further to around 60°.

Six inlet holes are provided for the air inlet with a diameter of 2 cm and three outlet holes with a diameter of 6 cm, which are joined to the drying cabinet. All sides of the dryer are painted black for the maximum heat trap inside the cabinet. The dryer's back view shows that the three trays consist of three different drying products. The bottom trays consist of woodchips, the middle one sawdust, and the top tray consists of the pellets. Table 1. depicts the design considerations considered in the experimental setup. These parameters are crucial for getting clear insights into the experiments and the various materials involved in the study.

The experiments were carried out for three days in the first week of October 2022. The whole body of the dryer and the collector is made of wooden blocks, and sealant was used to fill the gaps to avoid heat loss from the system. The body was coated with black paint to enhance heat absorptivity. Experiments were conducted during the prime sunshine hours of the day, i.e., 10 A.M. to 3 P.M. The highest radiation mainly was recorded between 12–1 P.M. Henceforth, the temperature rise inside the collector and dryer was also maximum during these hours. The anemometer measured the air inlet speed, which was controlled by the fan's speed at the top of the chimney. For all experiments, the air inlet speed was maintained at 2 m/s. An AC-powered fan was used at the top chimney to maintain this air flow rate. A multichannel data logger measured the temperature at six different locations of the inlet and outlets of the system. The relative humidity was measured using an (RH) meter valid in the range of 10–90%. The sample's initial and end weights and moisture content were measured on the weight and moisture balances. All these apparatuses were utilized to take measurements as per the required parameters described in the Section 2.

Table 1. Design items and descriptions considered during the experiments.

Item	Details	Units
Drying Products	Woodchips, Sawdust, Pellets	-
Weight of Product	1	kg for each
Duration of Experiment/day	10 A.M.–3 P.M.	h
Thickness of walls	2.5	cm
Thickness of collector glass	0.5	cm
Transmissivity of glass	0.89	Approx value
Number of trays	3	-
Holding tray	Metallic perforated	Material-Mild steel
Capacity of Dryer	180	L
Type of air flow	Forced Convection	AC power supply
Load capacity	6	kg
Drying time	5	h

2.2. Energy Analysis

The performance of the solar dryer is determined by the energy and exergy efficiency of the system. The efficiency of the dryer is coherent with the thermal efficiency of the solar air collector attached to the dryer. The temperature difference at the inlet T_i ($^{\circ}\text{C}$) and outlet T_o ($^{\circ}\text{C}$) of the collectors is used to calculate the useful heat energy Q_u of the collector, which is represented in Equation (1). C_p is the specific heat capacity of air at known temperature ($\text{kJ}/\text{kg}\cdot\text{K}$), and \dot{m} is the mass flow rate of air at a given temperature (kg/s) [31].

$$Q_u = \dot{m}C_p(T_o - T_i) \quad (2)$$

The mass flow rate can be calculated as the product of the air density ρ (Kg/m^3), average air velocity V (m/s) at the inlet of the collector, and the cross-section area $A_{collector}$ (m^2) of the duct [31,32].

$$\dot{m} = \rho VA_{collector} \quad (3)$$

The amount of solar radiation absorbed by the collector is the amount of heat input to the system. The heat input Q_I is the product of solar radiation I_T (W/m^2) falling on the collector and the surface area A_c (m^2) on which the radiation is falling [33]. Considering the transmissivity (τ) of the glass cover as 0.89 and assumed efficiency (η) of 0.9, I_T is the proportion of total incident radiation received (I_t) on the air collector [29].

$$Q_I = I_T A_c \quad (4)$$

The ratio of useful heat in the system to the input heat energy falling on the collector gives the thermal efficiency for the solar air collector. The thermal efficiency of the collector influences the temperature inside the drying chamber directly. The drying rate of the wood fuel enhances with better efficiency [33].

$$\eta_{th,c} = \frac{\dot{m}C_p(T_o - T_i)}{I_T A_c} \quad (5)$$

2.3. Exergy Analysis

The concept of exergy gain is based on the second law of thermodynamics. Thermal systems constitute available and unavailable energy parts known as “exergy” and “anergy”, respectively. Exergy efficiency is defined as the proportion of energy or exergy in the fuel utilized to make the product. Exergy analysis’s primary goal is to calculate the exergy destruction in various thermal system components [34]. The exergy gain can be defined

as the rise in exergy during the airflows inside the collector. Equation (5) gives the exergy increase, where $\frac{\rho_o}{\rho_i}$ is the ratio of air density at outlet and inlet, and R is the air gap Rayleigh number [35]. The inlet exergy depends on solar radiation and the absorbing surfaces [33]. The T_s temperature of solar intensity was considered as 5600 k, whereas T_a is the ambient temperature in Kelvin as the C_v is in (J/kg·K). The ratio of the increase in exergy outlet and the inlet gives the exergy efficiency. The dryer performs better with better exergy efficiency [33,36].

$$Ex_u = \dot{m} \left[C_p(T_o - T_i) - T_a \left(C_v \ln \left(\frac{T_o}{T_i} \right) - R \ln \left(\frac{\rho_o}{\rho_i} \right) \right) \right] \quad (6)$$

$$Ex_{in} = \left[1 + \frac{1}{3} \left(\frac{T_a}{T_s} \right)^4 - \frac{4}{3} \frac{T_a}{T_s} \right] I_T A_c \quad (7)$$

$$\eta_{th} = \frac{Ex_u}{Ex_{in}} \quad (8)$$

The type of material, the level of bound and unbound moisture, whether they are hygroscopic or non-hygroscopic, and the physical characteristics of the air utilized all impact how much moisture can be removed and then how efficiently. Non-hygroscopic materials can be dried to a moisture level of zero, whereas hygroscopic materials will always have some residual moisture. The moisture content (MC) helps plot the process's drying curve. The drying curve could be plotted MC (wet/dry) v/s time, drying rate v/s MC , or drying rate v/s time. In the experiments, MC was calculated on moisture (wet basis) using the moisture balance as the initial M_i and final M_f values pre- and post-experiment [37]. Additionally, the moisture ratio MR is calculated as the ratio of M_t (moisture content at any time) v/s M_o (moisture content initial) [38].

$$MC = \frac{(M_i - M_f)}{M_i} \cdot 100 \quad (9)$$

$$MR = \frac{M_t}{M_o} \quad (10)$$

The amount of moisture removed m_{water} (kg) can be calculated considering the mass of the product to be dried (m_i) (kg), and the heat required to evaporate the water is given as Q (KJ). $m_{water} h_{fg}$ represents consumed energy to evaporate water from the drying product [33]. The overall drying efficiency of the system is a ratio of v/s, as shown in Equation (12), where there are additional ways of heat source other than solar, which is not applicable in the present study.

$$m_{water} = \frac{m_i(M_i - M_f)}{(100 - M_f)} \quad (11)$$

$$Q = m_{water} h_{fg} \quad (12)$$

$$\eta_{system} = \frac{m_{water} h_{fg}}{I_T A_c + E} \quad (13)$$

2.4. Uncertainty Analysis

Analysis of uncertainty is used to identify the errors committed during the investigation. It is crucial to measure observed variances between measured values of an important parameter and its real value. The measurement uncertainties of all the linked independent variables are used to compute the uncertainty in a result [39]. In the present experimental setup, the weighing balance machine had accuracy of ± 0.1 gram. The humidity meter had $\pm 2.5\%$ of RH (relative humidity). The pyranometer had sensitivity of ± 0.1 mV/Wm². The moisture balance had readability of 0.001 gram. The anemometer gives accuracy of 0.1 m/s

in the working range of (0.3 to 20 m/s). All the measuring instruments were adequately calibrated before the experimental trials. The readings collected during measurements for this investigation were within an acceptable limit because the uncertainty values found during experimentation in the case of instrument performance were relatively minimal.

2.5. ANN Modelling

In recent times, artificial neural network (ANN) has evolved as useful computational software for modeling drying processes. Solar drying of various products involves various dependent variables, such as radiation, temperature, humidity, etc. Researchers worldwide use the ANN tool for testing and validation of the drying performance of solar dryers. The ANN-based models can predict the heat transfer coefficient [40], moisture ratio, moisture content, or drying rate depending on the requirements and available parameters [41]. Compared to other theoretical and practical modeling methodologies, ANNs may have advantages in simulating these devices, including high accuracy, generalization ability, and quick data insights [42]. Despite the basic assumptions in ANN-based modeling, using ANNs reduces solving complex mathematical models. In addition, fewer experiments are necessary to determine the input/output linkages compared to experimental investigations. Consequently, time and money could be saved by system modeling using ANNs. ANN processes the dataset fed into the system mathematically in the form of nodes/neurons. The model consists of input layers as the variables affecting the model, and the output layer is based on the output desired for the prediction. The researcher decides on the hidden layer of the model per the problem's intricacies. Training, validation, and testing are three stages of using ANN models. Training and validation stages involve both the input as well as target data. However, the testing is performed only with input data to see the model's suitability.

2.6. Structure of the ANN Model

The dryer's performance largely depends on the final moisture content of the dried product. It is helpful for researchers to develop a model to predict final moisture through neural network simulation. Bala et al. predicted the performance of the solar tunnel dryer using a multilayered neural network technique [43]. The model was trained using a backpropagation algorithm utilizing data on the solar drying of jackfruit bulbs and leather. Similarly, the present study is designed for the wood biofuels. Figure 2. depicts the ANN model developed for prediction of the final moisture content based on the experimental data collected during the experiments mentioned in Table 2. The five input variables affecting the process were selected as solar radiation, inlet and outlet temperature, and relative humidity. One hidden layer was selected in the model under Levenberg-Marquardt for training the mean square error regression in MATLAB2017b software. The Levenberg-Marquardt algorithm, which is created especially to minimize the sum of square error, is useful in similar predictions. As a first-choice supervised learning approach, the trainlm is frequently the quickest propagation algorithm in the toolbox, albeit it does use more memory than other algorithms [44]. It is applied in the current analysis. The model was trained with random data set from the experiments with 10,000 iterations with tan-sigmoid activation function for hidden neurons and purelin for linear output neurons. The test, train, and validation curves are presented in the Section 3. After several hits and trial runs, the best performance curve was plotted.

Table 2. Experimental parameter and their range considered for designing the ANN model.

Parameters	Range	Units
Solar Radiation	100–1100	W/m ²
Inlet Temperature	18–32	°C
Outlet Temperature	20–60	°C

Table 2. Cont.

Parameters	Range	Units
Initial Moisture content (wet basis)	32–36	%
Final moisture content (wet basis)	16–28	%
Relative Humidity	25–75	%



Figure 2. Experimental setup of the solar dryer for the investigations.

3. Experimental Results

The experiments were performed at the University of Miskolc, Hungary, on three sunny days in October 2022. The solar radiation measurements reflect the consistency of average radiation above 600 W/m^2 . However, sudden drops can be seen in the graph of Figure 3. The radiation values dropped suddenly because of the cloudiness or low sky-clarity index. Among the three-day experiments, the third day recorded the highest radiation value of 1100 W/m^2 . The consistency in good solar radiation helps in the rapid rise of temperature inside the collector and drying chamber, leading to better drying rates for the solar dryer.

Temperature rise is critical in the drying of agricultural products. The data logger and K-type thermocouple sensors were installed in the system at different locations. The collector's inlet and outlet temperature determine the air collector's efficiency. Considering no losses due to good insulation, the outlet temperature of the collector is the inlet of the drying chamber. In the three-day experiments, the maximum temperature achieved was $60 \text{ }^\circ\text{C}$ at around 1100 W/m^2 . The complete temperature rise was observed between 12–2 P.M. During total experimental hours, the temperature gradient between the ambient and inside the chamber was around $10 \text{ }^\circ\text{C}$, which aided in the continuous drying of the wood products. There was little temperature difference between the top layer and bottom layer of the drying chamber. However, the RH value differed by 4–5% occasionally. Figures 4–6 represent the temperature profile of the system for the testing hours during Days 1, 2, and 3, respectively.

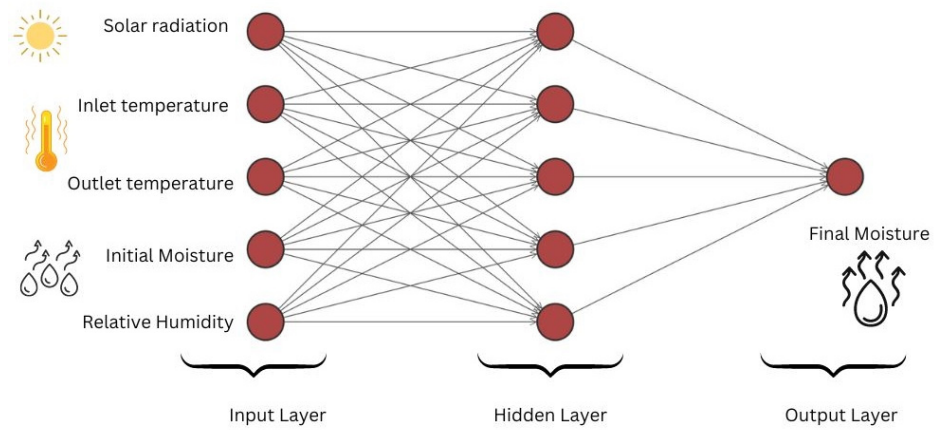


Figure 3. Optimized ANN architecture model developed for predicting the final moisture content.

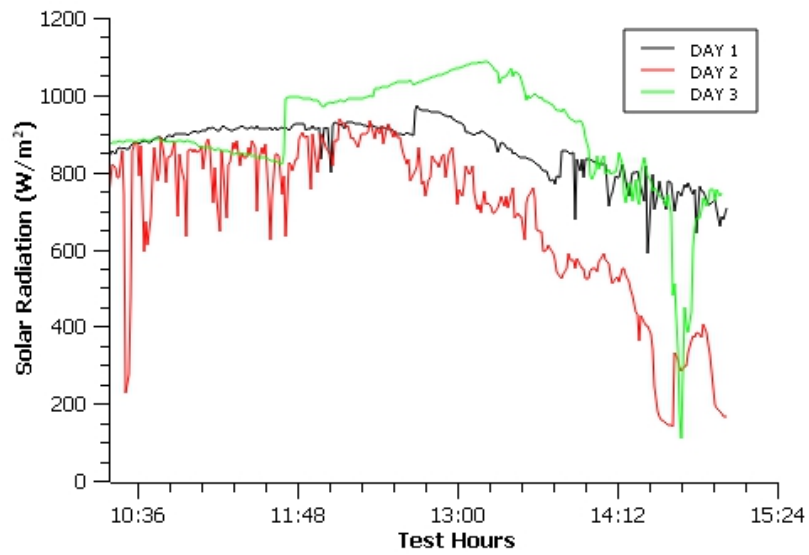


Figure 4. Solar radiation data collected for the three-day experimental setup.

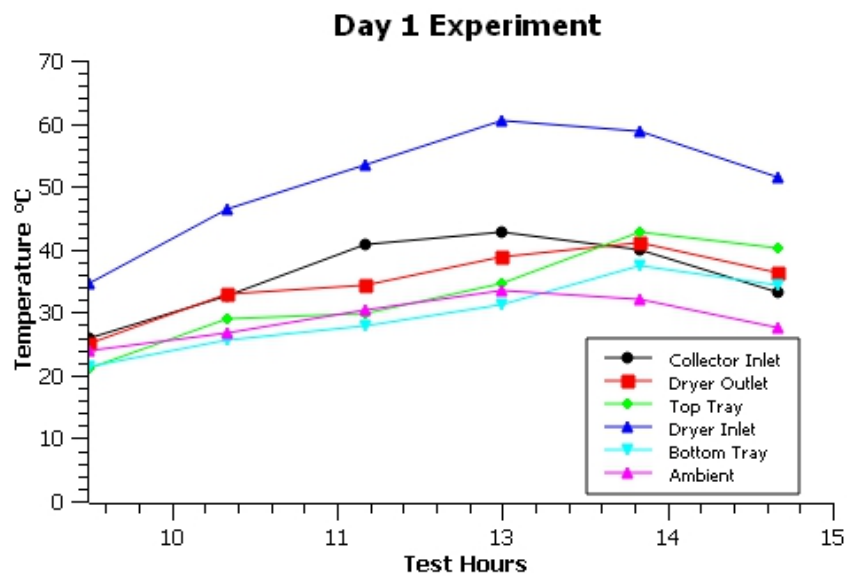


Figure 5. Temperature profiles for the first-day experimental setup of the dryer.

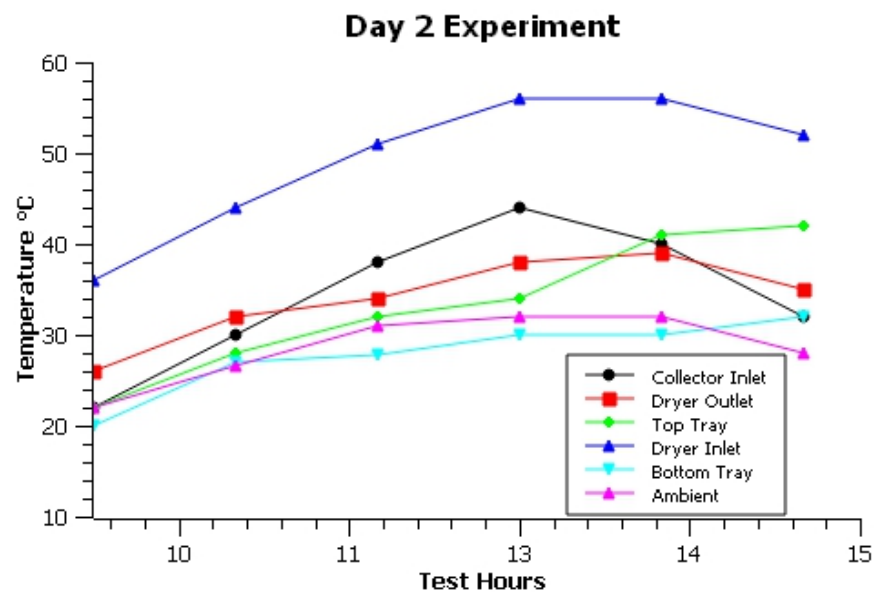


Figure 6. Temperature profiles for the second-day experimental setup of the dryer.

The instantaneous thermal efficiency of the air collector ranged 14.77% to 55%, as shown in Figure 7. The ambient temperature fluctuated between 18–32 °C. The thermal efficiency dropped between 11 A.M. and 1 P.M. However, the efficiency constantly rose after that period. The possible reason could be temperature stability was achieved during this period. Figure 8. depicts the variation of useful heat gains Q_u of the solar collectors and the ratio of the change in temperature (ΔT) to solar radiation ($^{\circ}\text{C m}^2/\text{W}$) with the drying time of the experiment. The ratio of (ΔT) to solar radiation ($^{\circ}\text{C m}^2/\text{W}$) was used as a basis to compare the trend shown in Figure 8. The hourly heat gain Q_u range was recorded as (201.65–420.55) watts. The total heat gain sum for Day1, 2 and 3 is 1495.57, 1663.62 and 2050.13 watts, respectively.

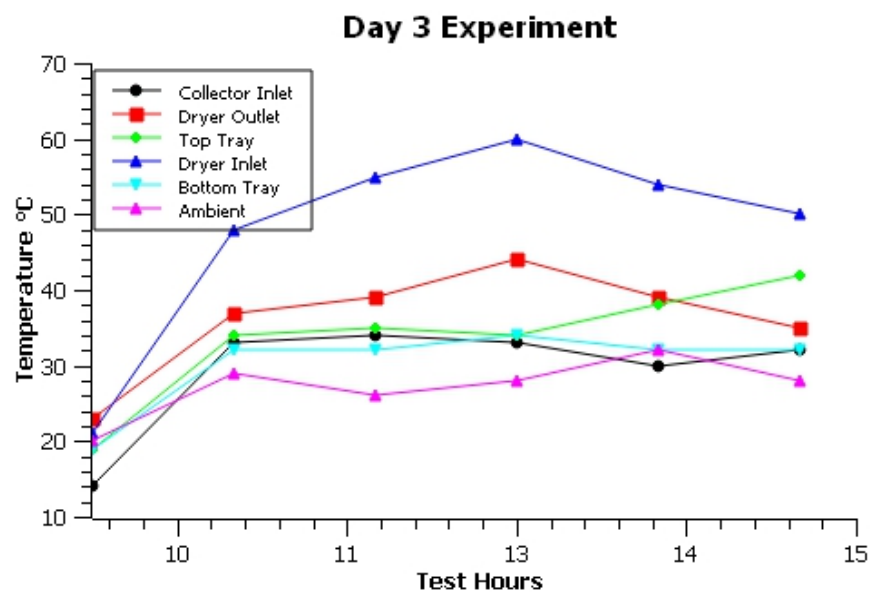


Figure 7. Temperature profiles for the third-day experimental setup of the dryer.

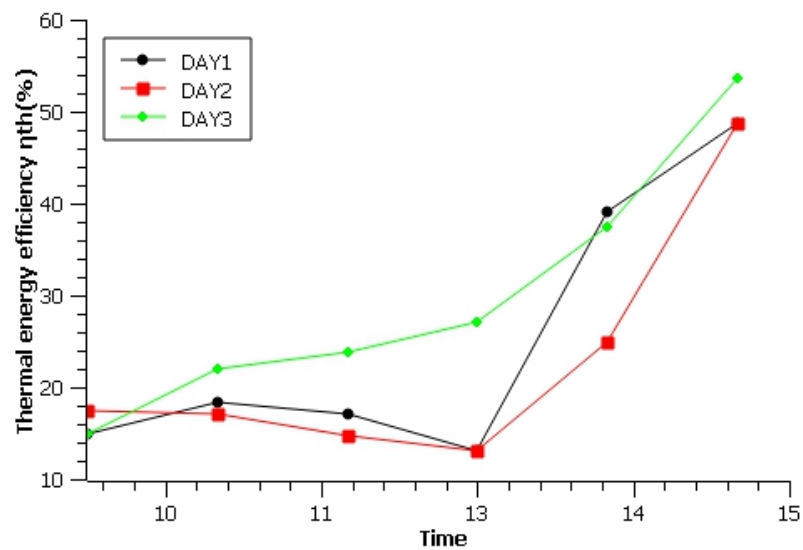


Figure 8. Thermal energy efficiency calculated on hourly basis for the three-days.

The exergy gain and the exergy efficiency calculations are critical in understanding the thermal performance of the air collector. The performance of the drying chamber is directly proportional to the collector's performance. The energy utilized or the gain improved from morning to afternoon hours, as indicated in Figure 9. The value of exergy gains enhanced from 76.26 watts to 408.57 watts during the experiments. The calculations were carried out as per the description of the study mentioned in Section 2.3. The exergy efficiency improved significantly from 4.8% to 51.1% from the first to the last hour, respectively as shown in Figure 10. In addition, the moisture ratio trends for the three wood fuels are plotted in Figure 11. The rapid loss of moisture content is evident in the wood pellets and sawdust samples. The high porosity level in these two fuel forms aids the fast internal migration of the surface water from the wood fuel. At the same time, the woodchip's surface water evaporation takes place slowly. Additionally, better exergy and long hours of continuous during can provide better results and insights on the drying behavior. The relative humidity (RH) measured for the samples during early hours was as high as 75%. However, the RH values kept fluctuating at the three levels of the tray primarily because of the different nature and drying rates of the three wood fuel samples.

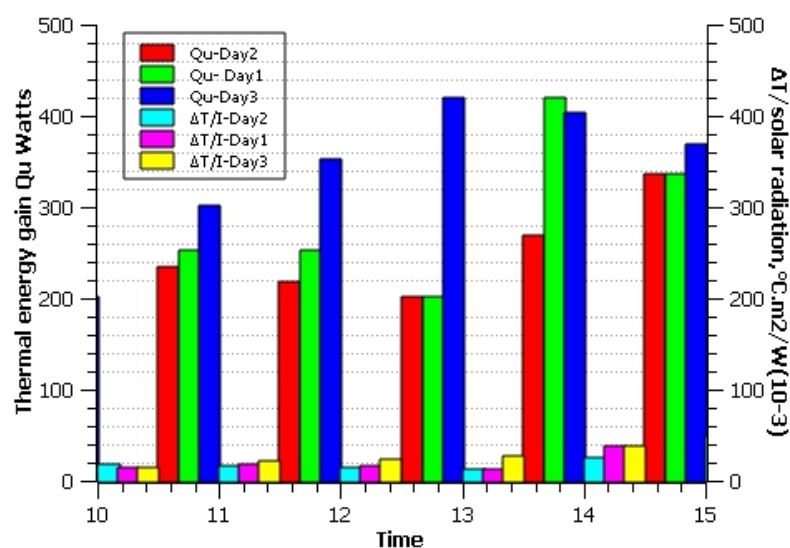


Figure 9. Thermal energy gain and the ΔT /solar radiation are calculated on an hourly basis.

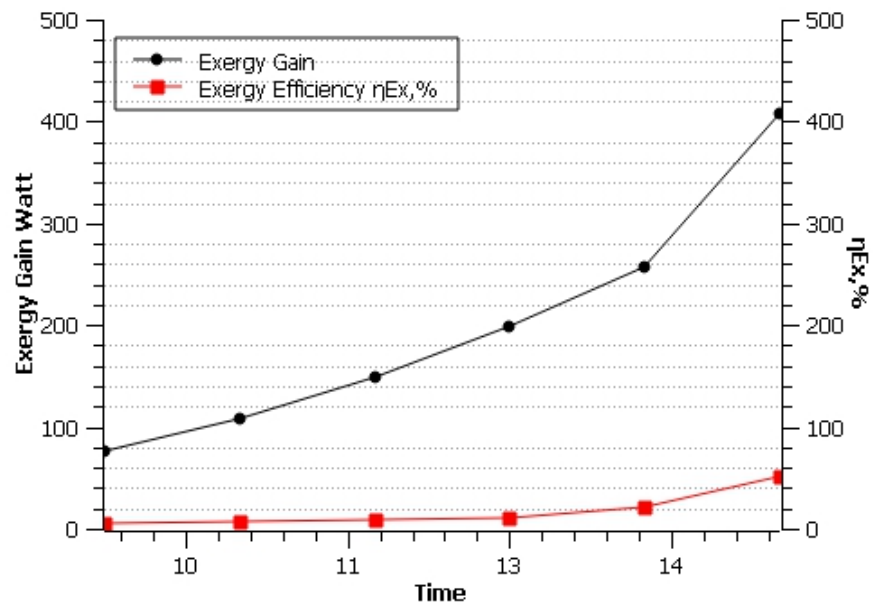


Figure 10. Exergy gain and exergy efficiency are calculated on an hourly basis.

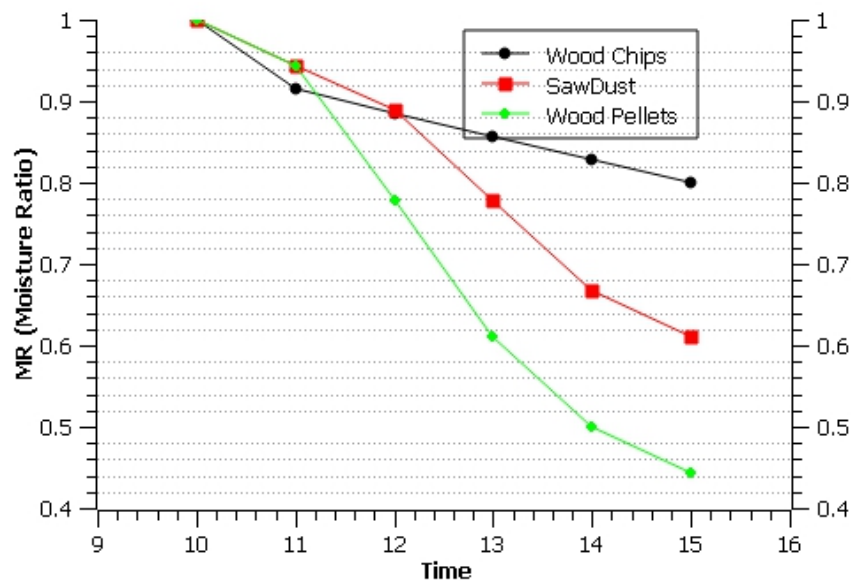


Figure 11. The moisture ratio was calculated for the wood chips, sawdust, and pellets.

The ANN model is explained in Section 2.4., and it was employed in the NN-tool of MATLAB software to validate and predict final moisture content. The coefficient of correlation (R) gives the goodness of the model. The best validation performance was 2.4949 at epoch 993, where the epoch measures the number of times all training vectors are used once to update the weights as shown in Figure 12. The training, validation, test, and overall values were found to be 1, 0.995, 0.970, and 0.990, reflecting the confirmation of the model shown in Figure 13. The predicted values were found to be coherent with the experimental dataset. The training was completed in 2nd iteration when the validation samples of mean square error reached the optimum value.

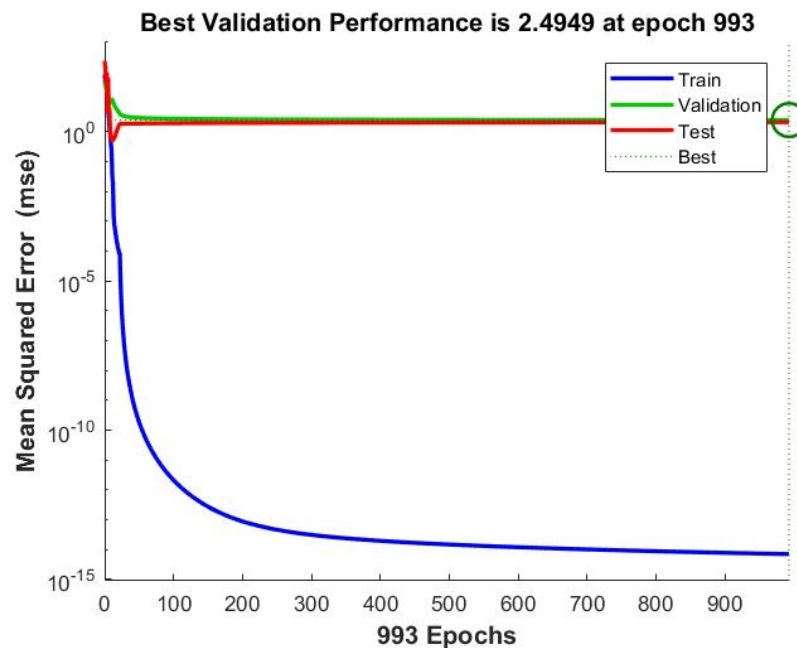


Figure 12. Root mean square error (MSE) plot for the ANN model.

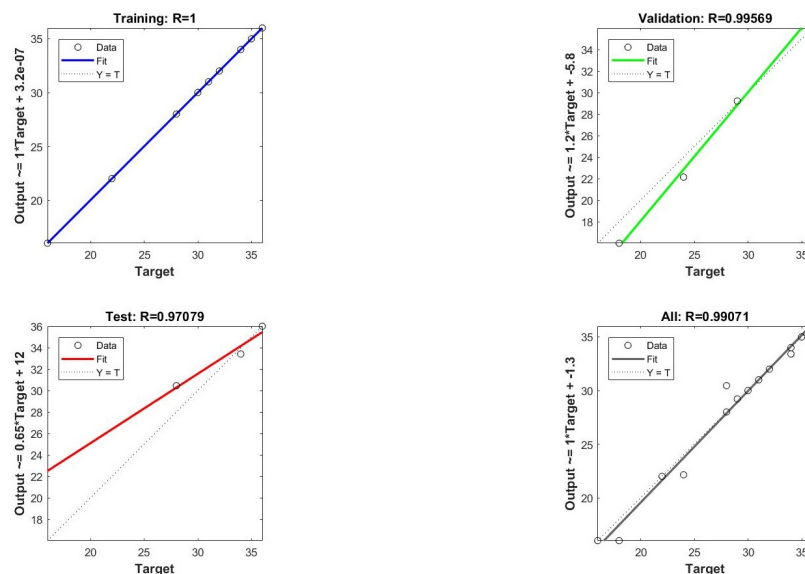


Figure 13. Regression plot for the ANN model after training the data.

4. Discussion

Biomass as a renewable energy source has its own geographical and technical limitations. Henceforth, a judicious and effective use of wood-based biofuels is inevitable. The storage of wood-based fuels, such as sawdust, pellets, and especially woodchips, is critical for large-scale consumption. The calorific value determines the fuel's quality and must be controlled. A lab-scale natural convective drier was previously developed and investigated for drying woodchips of grade (EN14961) [45]. On sunny winter days, the outlet's highest temperature was recorded to be 35 °C. It was noted that the moisture content did not go below 30% when drying in the open sun. Better results were obtained using the natural convection lab-scale direct-type box solar drier, which attained a moisture content of about 25% [46]. However, that study lacked consideration of several parameters, such as irradiance, airflow, etc.

Solar drying of wood with hybrid sources has emerged as a promising solution for proper storage with drying solutions [47]. A study by Raitila and Tsupari [4] found that solar drying with enhanced techniques could be profitable. Additionally, a payback time of 12–17 years in large-scale setups was estimated. Evacuated tube collectors have also been found efficient in reducing the payback period of drying systems for agricultural products [48]. Particularly, for solar wood dryers, Luis et al. even developed a model for designing dryers for rural communities considering the life cycle analysis and environmental impacts [49]. Sawdust is generally raw material for wood pellets. Investigations have been performed on microwave drying of sawdust [50]. However, the studies on solar drying solutions for sawdust or pellets are limited. In the present study, we found that the moisture removal from the three different wood fuels changed their color and texture. The before and after scenarios of the samples are presented in Figure 14. It is evident that the dark shade of the products became lighter after drying. The pellets become more brittle with higher moisture content. More than 35% of moisture content leads to brittle pellets. The sawdust and pellets had better drying rates than woodchips. However, the future direction of this research could be understanding the burning rates or emission controls with solar drying feasibility.



Figure 14. The sample's pictures were captured before and after drying during experiments.

5. Conclusions

The present work investigates the thermal performance of the forced convection solar cabinet dryer. The three different wood fuels were observed for drying using thermal energy from solar radiation. The inlet and outlet temperature difference lay between 10–20 °C for most of the test hours. The highest temperature recorded was 60 °C, with radiation of 1100 W/m². The use of wood for developing the outer body of the drier helped in better insulation of the system. The drying curves based on the moisture ratio reveal better drying rates for sawdust and pellets than woodchips. The maximum thermal energy and exergy efficiency observed during experimental hours as 55% and 51.1%, respectively. Sawdust and pellets had better drying rates than woodchips. The overall system efficiency of the dryer with respect to the woodchips, sawdust, and wood pellets was found to be (19.04–29.9)%, (23.34–33.2)%, and (21.11–31.1)% for the three days of experiments. An ANN model was created to predict the final moisture content for the system. The training, test,

and validation results of the optimized model are presented in the results section. A good coefficient of correlation (R) value revealed the model's suitability. The suitability of drying wood fuels with solar energy could be scaled for larger volumes with extra resources in the future. Investigations can also be carried out to understand the after-effects of drying on the large-scale drying, storage, combustion, and emission of wood fuels with hybridization of the dryer.

Author Contributions: Conceptualization, B.K., G.K. and Z.S.; methodology, B.K.; software, B.K.; validation, B.K., G.S. and G.K.; formal analysis, B.K.; investigation, B.K. and G.K.; resources, G.K.; data curation, B.K.; writing—original draft preparation, B.K.; writing—review and editing, B.K., Z.S. and G.S.; visualization, B.K.; supervision, Z.S. and G.S.; project administration, G.S. and G.K.; funding acquisition, Z.S. All authors have read and agreed to the published version of the manuscript.

Funding: This research received no external funding.

Institutional Review Board Statement: Not applicable.

Informed Consent Statement: Not applicable.

Data Availability Statement: Not applicable.

Acknowledgments: The research contributions from B.K. were conducted under the National Research, Development and Innovation Office (NKFIH), NKFIH Identifier: 135854.

Conflicts of Interest: The authors declare no conflict of interest.

References

1. Thees, O.; Erni, M.; Lemm, R.; Stadelmann, G.; Zenner, E.K. Future potentials of sustainable wood fuel from forests in Switzerland. *Biomass Bioenergy* **2020**, *141*, 105647. [CrossRef]
2. Yi, J.; Li, X.; He, J.; Duan, X. Drying efficiency and product quality of biomass drying: A review. *Dry Technol.* **2020**, *38*, 2039–2054. [CrossRef]
3. Silva, J.; Ferreira, A.; Teixeira, S.; Martins, L.; Ferreira, E.; Teixeira, J.C. Sawdust drying process in a large-scale pellets facility: An energy and exergy analysis. *Clean. Environ. Syst.* **2021**, *2*, 100037. [CrossRef]
4. Raitila, J.; Tsupari, E. Feasibility of Solar-Enhanced Drying of Woody Biomass. *BioEnergy Res.* **2020**, *13*, 210–221. [CrossRef]
5. Hosseini, S.M.; Peer, A. Wood Products Manufacturing Optimization: A Survey. *IEEE Access* **2022**, *10*, 121653–121683. [CrossRef]
6. Meng, Y.; Chen, G.; Hong, G.; Wang, M.; Gao, J.; Chen, Y. Energy efficiency performance enhancement of industrial conventional wood drying kiln by adding forced ventilation and waste heat recovery system: A comparative study. *Maderas Cienc. Tecnol.* **2019**, *21*, 545–558. [CrossRef]
7. Lamrani, B.; Bekkioui, N.; Simo-Tagne, M.; Ndukwu, M.C. Recent progress in solar wood drying: An updated review. *Dry. Technol.* **2022**, *2022*, 2112048. [CrossRef]
8. Rudra Solar Energy. Available online: <https://www.rudrasolarenergy.com/> (accessed on 4 January 2023).
9. S. Kiln Kit, Wood Mizer. Available online: <https://woodmizer.com.au/> (accessed on 4 January 2023).
10. Hangzhou Tech Drying Equipment CO., LTD. Solar Wood Drying Kiln. Available online: <https://www.wooddryingequipment.com/> (accessed on 4 January 2023).
11. Solar Dryers Australia Pty LTD. Available online: <http://www.solardry.com.au/solardry/index.html> (accessed on 5 January 2023).
12. Kumar, B.; Berényi, L.; Szamosi, Z.; Szepesi, G.L. Business model analysis for the scope of entrepreneurship in a solar drying field in the European region. In *Entrepreneurship in the Raw Materials Sector*; CRC Press: Boca Raton, FL, USA, 2022; pp. 85–92. [CrossRef]
13. Sehwat, R.; Chandra, A.; Nema, P.; Kumar, V. Drying of Fruits and Vegetables in a Developed Multimode Drying Unit and Comparison with Commercially Available Systems. *J. Inst. Eng. Ser. A* **2019**, *100*, 381–386. [CrossRef]
14. Alakoski, E.; Jämsén, M.; Agar, D.; Tampio, E.; Wihersaari, M. From wood pellets to wood chips, risks of degradation and emissions from the storage of woody biomass—A short review. *Renew. Sustain. Energy Rev.* **2016**, *54*, 376–383. [CrossRef]
15. Stasiak, M.; Molenda, M.; Bańda, M.; Gondek, E. Mechanical properties of sawdust and woodchips. *Fuel* **2015**, *159*, 900–908. [CrossRef]
16. Stenström, S. Drying of biofuels from the forest—A review. *Dry. Technol.* **2017**, *35*, 1167–1181. [CrossRef]
17. Perea-Moreno, A.-J.; Juaidi, A.; Manzano-Agugliaro, F. Solar greenhouse dryer system for wood chips improvement as biofuel. *J. Clean. Prod.* **2016**, *135*, 1233–1241. [CrossRef]
18. Khouya, A. Modelling and analysis of a hybrid solar dryer for woody biomass. *Energy* **2021**, *216*, 119287. [CrossRef]
19. Reyes, A.; Gatica, E.; Henríquez-Vargas, L.; Pailahueque, N. Modeling of sawdust drying in spouted beds using solar energy and phase change materials. *J. Energy Storage* **2022**, *51*, 104441. [CrossRef]

20. Almeida, D.; Marques, E. Solar Drying Acacia—Influence in Pellets Quality: Experimental Results. In Proceedings of the COBEM 2013, 22nd International Congress of Mechanical Engineering, Ribeirão Preto, Spain; 2013; pp. 6742–6752.
21. Ndukwu, M.C.; Bennamoun, L. Potential of integrating Na₂SO₄ · 10H₂O pellets in solar drying system. *Dry. Technol.* **2018**, *36*, 1017–1030. [CrossRef]
22. Simo-Tagne, M.; Bennamoun, L. Numerical study of timber solar drying with application to different geographical and climatic conditions in Central Africa. *Sol. Energy* **2018**, *170*, 454–469. [CrossRef]
23. Awadalla, H.S.F.; El-Dib, A.; Mohamad, M.; Reuss, M.; Hussein, H.M.S. Mathematical modelling and experimental verification of wood drying process. *Energy Convers. Manag.* **2004**, *45*, 197–207. [CrossRef]
24. Güler, H.Ö.; Sözen, A.; Tuncer, A.D.; Afshari, F.; Khanlari, A.; Şirin, C.; Gungor, A. Experimental and CFD survey of indirect solar dryer modified with low-cost iron mesh. *Sol. Energy* **2020**, *197*, 371–384. [CrossRef]
25. UNECE. Wood energy on the rise in Europe. *Press Release*. Available online: https://unece.org/climate-change/press/wood-energy-rise-europe#:~:text=Countries_in_the_European_Union,increased_demand_byindividual_households (accessed on 5 December 2022).
26. Kumar, B.; Szepesi, G.; Čonka, Z.; Kolcun, M.; Péter, Z.; Berényi, L.; Szamosi, Z. Trendline assessment of solar energy potential in hungary and current scenario of renewable energy in the visegrád countries for future sustainability. *Sustainability* **2021**, *13*, 5462. [CrossRef]
27. Khouya, A. Energy analysis of a combined solar wood drying system. *Sol. Energy* **2022**, *231*, 270–282. [CrossRef]
28. Blanco-Cano, L.; Soria-Verdugo, A.; Garcia-Gutierrez, L.; Ruiz-Rivas, U. Evaluation of the Maximum Evaporation Rate in Small-Scale Indirect Solar Dryers. *J. Sol. Energy Eng. Trans. ASME* **2016**, *138*, 1–4. [CrossRef]
29. Babar, O.A.; Tarafdar, A.; Malakar, S.; Arora, V.; Nema, P.K. Design and performance evaluation of a passive flat plate collector solar dryer for agricultural products. *J. Food Process Eng.* **2020**, *43*, e13484. [CrossRef]
30. Alamu, O.J.; Nwaokocho, C.; Adunola, O. Design and Construction of a Domestic Passive Solar Food Dryer. *Leonardo J. Sci.* **2010**, *16*, 71–82.
31. Esen, H. Experimental energy and exergy analysis of a double-flow solar air heater having different obstacles on absorber plates. *Build. Environ.* **2008**, *43*, 1046–1054. [CrossRef]
32. Kurtbas, A.; Durmus, A. Efficiency and exergy analysis of a new solar air heater. *Renew. Energy* **2004**, *29*, 1489–1501. [CrossRef]
33. Habtay, G.; Al-Neama, M.; Buzas, J.; Farkas, I. Experimental Performance of Solar Air Heaters for Drying Applications. *Eur. J. Energy Res.* **2021**, *1*, 4–10. [CrossRef]
34. Hatami, S.; Payganeh, G.; Mehrpanahi, A. Energy and exergy analysis of an indirect solar dryer based on a dynamic model. *J. Clean. Prod.* **2020**, *244*, 118809. [CrossRef]
35. Bahrehmand, D.; Ameri, M.; Gholampour, M. Energy and exergy analysis of different solar air collector systems with forced convection. *Renew. Energy* **2015**, *83*, 1119–1130. [CrossRef]
36. Abdelkader, T.K.; Fan, Q.; Gaballah, E.; Wang, S.; Zhang, Y. Energy and Exergy Analysis of a Flat-Plate Solar Air Heater Artificially Roughened and Coated with a Novel Solar Selective Coating. *Energies* **2020**, *13*, 997. [CrossRef]
37. Krabch, H.; Tadili, R.; Idrissi, A. Design, realization and comparison of three passive solar dryers. Orange drying application for the Rabat site (Morocco). *Results Eng.* **2022**, *15*, 100532. [CrossRef]
38. Sharabiani, V.R.; Kaveh, M.; Abdi, R.; Szymanek, M.; Tanaś, W. Estimation of moisture ratio for apple drying by convective and microwave methods using artificial neural network modeling. *Sci. Rep.* **2021**, *11*, 9155. [CrossRef] [PubMed]
39. Singh, P.P.; Singh, S.; Dhaliwal, S.S. Multi-shelf domestic solar dryer. *Energy Convers. Manag.* **2006**, *47*, 1799–1815. [CrossRef]
40. Kushwah, A.K.; Gaur, M.; Kumar, A.; Singh, P.S. Application of ANN and prediction of drying behavior of mushroom drying in side hybrid greenhouse solar dryer: An experimental validation. *J. Therm. Eng.* **2022**, *8*, 221–234. [CrossRef]
41. Sadadou, A.; Hanini, S.; Laidi, M.; Rezrazi, A. ANN-based Approach to Model MC/DR of Some Fruits Under Solar Drying. *J. Chem. Chem. Eng.* **2021**, *70*, 233–242. [CrossRef]
42. Elsheikh, A.H.; Sharshir, S.; Elaziz, M.A.; Kabeel, A.; Guilan, W.; Haiou, Z. Modeling of solar energy systems using artificial neural network: A comprehensive review. *Sol. Energy* **2019**, *180*, 622–639. [CrossRef]
43. Bala, B.K.; Ashraf, M.; Uddin, M.; Janjai, S. Experimental and neural network prediction of the performance of a solar tunnel drier for drying jackfruit bulbs and leather. *J. Food Process Eng.* **2005**, *28*, 552–566. [CrossRef]
44. Tiwari, S. ANN and mathematical modelling for moisture evaporation with thermal modelling of bitter gourd flakes drying in SPVT solar dryer. *Heat Mass Transf.* **2020**, *56*, 2831–2845. [CrossRef]
45. Kumar, B.; Szepesi, L.; Szamosi, Z. Drying behaviour observations for wood chips of grade EN14961. *Multidiscip. Tudományok* **2021**, *11*, 151–156. [CrossRef]
46. Baibhaw, K.; Szepesi, G.; Szamosi, Z. Design and Development of natural convective solar dryer. *Multidiscip. Sci.* **2021**, *11*, 144–150. [CrossRef]
47. Lamrani, B.; Draoui, A. Thermal performance and economic analysis of an indirect solar dryer of wood integrated with packed-bed thermal energy storage system: A case study of solar thermal applications. *Dry. Technol.* **2021**, *39*, 1371–1388. [CrossRef]
48. Malakar, S.; Arora, V.; Nema, P.K. Design and performance evaluation of an evacuated tube solar dryer for drying garlic clove. *Renew. Energy* **2021**, *168*, 568–580. [CrossRef]

49. López-Sosa, L.B.; Núñez-González, J.; Beltrán, A.; Morales-Máximo, M.; Morales-Sánchez, M.; Serrano-Medrano, M.; García, C.A. A New Methodology for the Development of Appropriate Technology: A Case Study for the Development of a Wood Solar Dryer. *Sustainability* **2019**, *11*, 5620. [[CrossRef](#)]
50. Bhattarai, S.; Oh, J.; Choi, Y.; Oh, K.; Euh, S.; Kim, D.H. Microwave Drying of Sawdust for Pellet Production: Kinetic Study under Batch Mode. *J. Biosyst. Eng.* **2012**, *37*, 385–397. [[CrossRef](#)]

Disclaimer/Publisher’s Note: The statements, opinions and data contained in all publications are solely those of the individual author(s) and contributor(s) and not of MDPI and/or the editor(s). MDPI and/or the editor(s) disclaim responsibility for any injury to people or property resulting from any ideas, methods, instructions or products referred to in the content.